

SANDIA REPORT

SAND2008-7180

Unlimited Release

Printed November, 2008

Medically Relevant ElectroNeedle™ Technology Development

Komandoor Achyuthan, Jason Harper, Jaime McClain, Carrie Schmidt, Gregory Ten Eyck and

Michael Thomas

Prepared by
Sandia National Laboratories
Albuquerque, New Mexico 87185 and Livermore, California 94550

Sandia is a multiprogram laboratory operated by Sandia Corporation,
a Lockheed Martin Company, for the United States Department of Energy's
National Nuclear Security Administration under Contract DE-AC04-94AL85000.

Approved for public release; further dissemination unlimited.



Issued by Sandia National Laboratories, operated for the United States Department of Energy by Sandia Corporation.

NOTICE: This report was prepared as an account of work sponsored by an agency of the United States Government. Neither the United States Government, nor any agency thereof, nor any of their employees, nor any of their contractors, subcontractors, or their employees, make any warranty, express or implied, or assume any legal liability or responsibility for the accuracy, completeness, or usefulness of any information, apparatus, product, or process disclosed, or represent that its use would not infringe privately owned rights. Reference herein to any specific commercial product, process, or service by trade name, trademark, manufacturer, or otherwise, does not necessarily constitute or imply its endorsement, recommendation, or favoring by the United States Government, any agency thereof, or any of their contractors or subcontractors. The views and opinions expressed herein do not necessarily state or reflect those of the United States Government, any agency thereof, or any of their contractors.

Printed in the United States of America. This report has been reproduced directly from the best available copy.

Available to DOE and DOE contractors from
U.S. Department of Energy
Office of Scientific and Technical Information
P.O. Box 62
Oak Ridge, TN 37831

Telephone: (865) 576-8401
Facsimile: (865) 576-5728
E-Mail: reports@adonis.osti.gov
Online ordering: <http://www.osti.gov/bridge>

Available to the public from
U.S. Department of Commerce
National Technical Information Service
5285 Port Royal Rd.
Springfield, VA 22161

Telephone: (800) 553-6847
Facsimile: (703) 605-6900
E-Mail: orders@ntis.fedworld.gov
Online order: <http://www.ntis.gov/help/ordermethods.asp?loc=7-4-0#online>



SAND-2008-7180

Unlimited Release

Printed November 2008

Medically Relevant ElectroNeedle™ Technology Development

Komandoor Achyuthan, Jason Harper, Michael Thomas (Biosensors and Nanomaterials, 01714)

Jaime McClain (MEMS Core Technologies, 017491)

Carrie Schmidt and Gregory Ten Eyck (Integrated Microdevice System, 01717)

Sandia National Laboratories P.O. Box 5800 Albuquerque, New Mexico 87185-MS1080

Abstract

ElectroNeedles technology was developed as part of an earlier Grand Challenge effort on Bio-Micro Fuel Cell project. During this earlier work, the fabrication of the ElectroNeedles was accomplished along with proof-of-concept work on several electrochemically active analytes such as glucose, quinone and ferricyanide. Additionally, earlier work demonstrated technology potential in the field of immunosensors by specifically detecting Troponin, a cardiac biomarker. The current work focused upon fabrication process reproducibility of the ElectroNeedles and then using the devices to sensitively detect *p*-cresol, a biomarker for kidney failure or nephrotoxicity. Valuable lessons were learned regarding fabrication assurance and quality. The detection of *p*-cresol was accomplished by electrochemistry as well as using fluorescence to benchmark ElectroNeedles performance. Results from these studies will serve as a guide for the future fabrication processes involving ElectroNeedles as well as provide the groundwork necessary to expand technology applications. **One paper has been accepted for publication acknowledging LDRD funding (K. E. Achyuthan *et al*, Comb. Chem. & HTS, 2008).** We are exploring the scope for a second paper describing the applications potential of this technology.

ACKNOWLEDGMENTS

We thank Drs. Stephen Caslanuovo, Kent Schubert and Wahid Hermina for their strong support of this project, and David Ingersoll and Graham Yelton for expert advice on electrochemical measurements and ElectroNeedles technology and Dr. Dominic Raj for suggesting *p*-Cresol as a biomarker for kidney toxicity. Diazonium based electrode surface modification was developed and characterized by the David R. Wheeler and Susan M. Brozik labs at Sandia National Laboratories. We thank Dr. Paul Galambos for critical comments on the SAND report.

Sandia National Laboratories is a multiprogram laboratory operated by Sandia Corporation, a Lockheed Martin Company, for the United States Department of Energy under contract DE-ACO4-94-AL85000.

CONTENTS

1. Introduction.....	8
2. ElectroNeedles Array Fabrication.....	9
3. Device Fabrication.....	10
4. Lessons Learned.....	12
5. <i>p</i> -Cresol – a uremic toxin and our target analyte.....	12
6. Electrochemical detection of <i>p</i> -Cresol by two Investigators.....	12
6.1 Investigator # 1.....	12
6.2 Investigator # 2.....	16
7. <i>p</i> -Cresol detection using enzyme catalysis.....	20
8. Fluorescent properties of oxidized <i>p</i> -Cresol.....	20
9. Concluding Remarks.....	21
10. References.....	22
11. Distribution.....	23

FIGURES

Figure-1:	Approach to a minimally invasive electrochemical assay.....	8
Figure-2:	ElectroNeedles Fabrication.....	9
Figure-3:	General sequence of FOTURAN exposure and baking.....	10
Figures-4A & B:	1mM <i>p</i> -Cresol and 100µM <i>p</i> -Cresol electrochemical assay.....	13
Figures-4C & 5A:	1µM <i>p</i> -Cresol and 1nM <i>p</i> -Cresol electrochemical assay.....	14
Figures-5B & 5C:	1µM <i>p</i> -Cresol and 100µM <i>p</i> -Cresol electrochemical assay.....	15
Figure-6:	Mechanism of diazonium assembly onto electrode surfaces.....	17
Figure-7:	Cyclic voltammograms showing <i>p</i> -Cresol oxidation at different Au electrode Surfaces.....	18
Figure-8:	Sequential cyclic voltammograms scans of an aminophenyl thin film Modified Au electrode.....	19
Figure-9:	Oxidative <i>p</i> -Cresol detection at an aminophenyl thin film modified Au Electrode.....	19
Figure-10:	Excitation and emission profiles of the laccase-catalyzed oxidation Products of <i>p</i> -Cresol.....	20
Figure-11:	<i>p</i> -Cresol affinity for laccase.....	21

NOMENCLATURE

DOE	Department of Energy
DTRA-JSTO	Defense Threat Reduction Agency-Joint Science & Technology Office
HTS	High-throughput screening
LDRD	Laboratory Directed Research and Development
SNL	Sandia National Laboratories

1.0 INTRODUCTION

There is a need for the sensitive detection of chem.-bio agents for military and national security applications. There also exists a need for rapid, inexpensive and field deployable diagnostic device capable of complementing timely therapeutics for both human and agricultural/animal diseases. Current methods of diagnostics are not suitable for screening large populations nor do they lend themselves easily to point-of-care diagnostics such as first responders, battlefield or a physician's office. To address these problems we have been developing the ElectroNeedles technology in two distinct platforms: ElectroNeedles and μ Posts. The groundwork for these studies was laid previously through a Bio-Micro Fuel Cell Grand Challenge and is being continued under the auspices of this late-start LDRD. Our approach is shown below. In this LDRD work, we utilized these technologies to sensitively measure *p*-Cresol, a uremic toxin. We compare the contrast electrochemical measurements using ElectroNeedles with a high-throughput screening (HTS) fluorescent assay. Our data might be useful for developing the ElectroNeedles technology for rapid diagnostic testing of kidney failure and in the triage of kidney dialysis patients.

Our Approach

A minimally invasive sensor placed against the skin capable of performing electrochemical immunoassays just beneath the skin's surface -

- arrays of microfabricated metal posts (ElectroNeedles™)
- post height adjusted to penetrate epidermal or dermal layers
- tips of posts functionalized with electrochemically-active ligands
- epidermal posts sample small molecules (e.g., glucose) in interstitial cellular fluid
- dermal posts sample large molecules (e.g., proteins) in blood
- real-time readout of electrochemical response

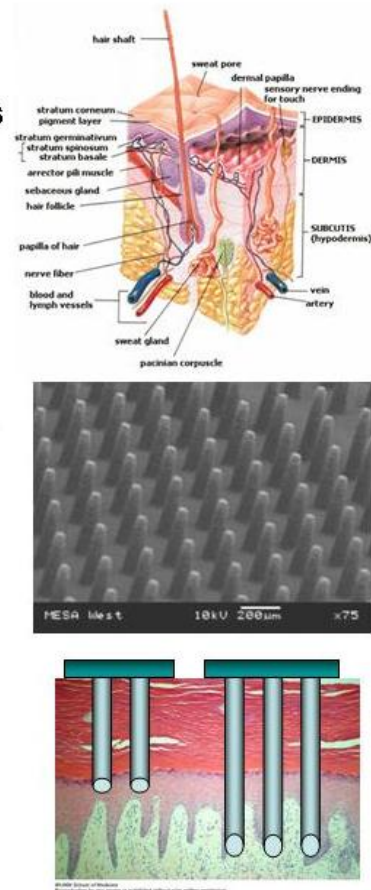


Figure-1: Approach to a minimally invasive electrochemical sensor array

2.0 ElectroNeedles Array Fabrication

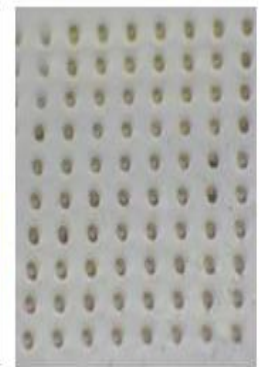
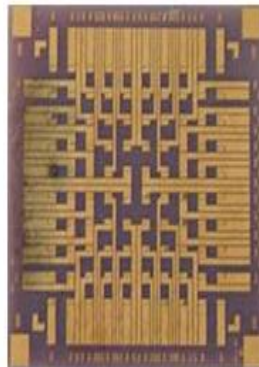
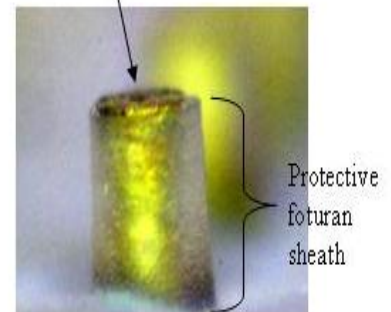
The highlights of our approach toward fabrication of the ElectroNeedles are shown in the figure below:

ElectroNeedle Arrays

- Form hollow microneedles in photo-patternable glass substrate
- Characteristic dimension - 100 microns
- Electroplate gold through hollow needle core
- 5 X 5 and 10 X10 arrays
- Individual electrical connection to each microneedle from the back of the substrate
- Arrays fabricated in Sandia's MESA Microsystems facility



Exposed electrode surface



Backside electrical contacts

Figure-2: ElectroNeedles Fabrication

3.0 DEVICE FABRICATION

The fabrication of microneedles involves several distinct processing phases and is based on a platform of photopatternable glass. In the present case the glass used is FOTURAN, provided by Mikroglas Chemtech GmbH. The general process flow for fabrication is to pattern and etch *via* holes through the glass, $\sim 100\mu\text{m}$ *dia.* and on a 1mm pitch. These etched holes are filled with gold by means of electroplating. Both faces are polished to remove plating overburden and give a clean working surface for further processing. The wafer is baked for a second time to activate the glass for the etch that forms the needle protrusions. A backside metallization is applied using standard liftoff techniques that provides the interconnections between the needles and bond pads used in packaging. At this point, a second etch is performed on the front side of the glass to form the protruding needles. The wafers are then diced into roughly 1cm x 1cm die which are then wirebonded in a custom carrier that has a machined hole to expose the needles.

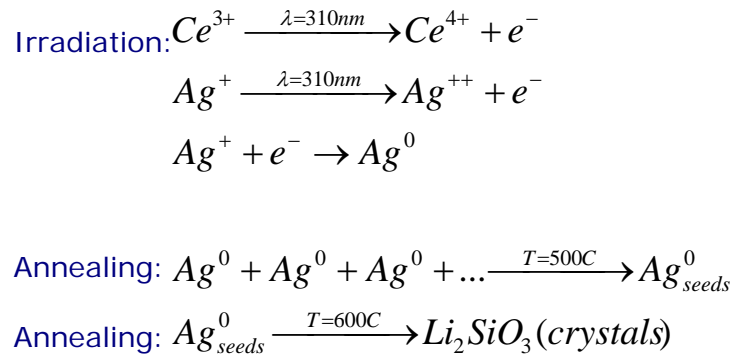


Figure-3: General sequence of FOTURAN exposure and baking

FOTURAN patterning is accomplished through the use of UV light (310nm) and several bake cycles followed by etching in an acid bath. The general sequence for exposure and baking is shown in Figure 3. The glass contains Ce^{3+} ions and Ag_2O in its matrix. The UV light ionizes the Ce and the freed electrons reduce Ag^{+} to Ag^0 . These Ag seeds agglomerate during the first baking cycle and serve as nucleation centers for Li_2SiO_3 crystal growth during the second annealing step. These Li_2SiO_3 crystals etch faster in HF giving the selectivity needed to pattern features into the bulk of the glass (in this case vias). The intensity of the light reaching a given point (depth) in the glass is based on both the absorption of the glass itself and the interaction between the photons and the Ce^{3+} and Ag^{+} embedded in the glass. Additional scattering losses also factor into this. The Ag^{+} oxidation state is not changed by thermal treatment so no additional nuclei form during the thermal treatment. Ag clusters formed in early part of heat treatment are a few hundred atoms in size and their size do not depend distinctly on temperature but increase with added exposure time [1]. Therefore there is an important balance between the exposure energy and bake conditions to produce uniform highly anisotropic features.

For this work, a total of seven wafers were processed through various stages. In all cases, the FOTURAN used was 1.1mm thick. This thickness allowed a sufficiently robust base of glass to remain once the needle protrusions were formed. The FOTURAN was placed into a UV flood exposure tool optimized for 310nm light and exposed through a quartz photomask. The flux for the system was measured to be 30 mW/cm^2 , and each exposure lasted for 25 minutes giving a

total dose of 45 J/cm^2 . The exposed wafers were baked in an oven at $500 \text{ }^\circ\text{C}$ for 1 hour 15 minutes and then again at $600 \text{ }^\circ\text{C}$ for an additional 1 hr and 15 minutes. After baking the exposed regions are dark brown and easily seen. This contrast allowed a second mask to be aligned to pattern the protruded needles and define the sheath thickness. The wafers were again exposed at 30 mW/cm^2 but the second exposure lasted for only 15 minutes. This shorter exposure allowed the top of the wafer to be etched at a much higher rate than the bottom. The wafers were then etched in a 10:1:1 $\text{H}_2\text{O}:\text{HF}:\text{HNO}_3$ solution in an ultrasonic bath for 45 minutes. This etch created the *via* holes but did not attack the front surface of the wafer (from 2nd exposure) because the exposed glass had not been baked.

The next phase of the processing was the *via* hole fill with electroplated gold. Successful electroplating requires a seed layer at the bottom of each *via* that will support a uniform current density across the wafer. The most reliable method for this is to metalize the backside of the wafer (200\AA Ti / 200\AA Pt / 1000\AA Au) and bond it to a support structure also coated with metal. The sandwiched metal layer serves as the seed for the electroplating, but because it is only exposed to the bath through the *via* holes the plating is confined to the *vias*. Ideally, a glancing angle deposition would be used for coating the backside of the FOTURAN to minimize the metal deposition on the sidewalls of the *vias*. Non-uniform coating on the *via* sidewalls can lead to gaps in the plated posts. Unfortunately, the wafers in this project were metalized using liftoff tooling so a significant portion of the *via* sidewalls were coated, ultimately complicating the plating. Because the FOTURAN wafers have a relatively large bow/warp characteristic ($>40\mu\text{m}$) that is exacerbated by the bake cycle near the glass melting point, the wafers must be planarized before attempting to bond them. This is typically accomplished by lapping. Because of difficulties with the lapping facilities the wafers were not lapped before the backside metal was applied, so several bonding strategies were explored to mitigate the risks. Five of the seven wafers were metalized at this stage of the processing (2 wafers remain that have been patterned and etched but not metalized).

The first wafer was bonded to 3MTM Conductive Gold Fabric Tape (AU-2190). The bond appeared successful and the wafer did not crack when cooled, but the electroplating was unsuccessful. The second wafer was bonded to a sheet of $25\mu\text{m}$ thick Ti foil coated on one side with Ti/Pt/Au. This wafer was then sealed into a plating fixture to avoid backside plating. Again, the bond appeared to be successful but only 3 of the die across the wafer plated. These die were able to be further processed into completed devices. The next 2 wafers were bonded to Ti/Pt/Au coated Polyimide sheets and again the bonding appeared to be successful. One of these wafers was partially plated and looked promising. Unfortunately the Polyimide was removed from the backside before the plating was completed so this wafer now contains only partially filled *vias*. The other wafer was plated for 40 hours but the bond was not strong enough and the Polyimide delaminated. The backside metal remaining was non-uniform so this wafer requires lapping/polishing of backside before it can be re-metalized and bonded to complete the plating.

The final wafer was bonded to a Ti/Pt/Au coated Si wafer, and as expected it shattered as the bond cooled. The wafer contained a few unbroken die so it was put into the plating bath but the plating was largely unsuccessful because of non-uniform current density on the seed and/or a lack of solution wetting in the holes at the start of plating. Ultimately 3 die appeared to be partially plated and they were further processed into packaged pieces.

A total of 4 die were plated with solid *vias* and 2 were plated that had hollow centers. Each of these was cleaned by shaving off the plating overburden, hand-polishing, baked at 500C for 1 hour then at 600C for an additional hour. Liftoff patterning was performed to apply the backside metallization interconnect pattern. These die were then mounted with crystal bond to a Si support wafer so that they could be etched to form the needle protrusions. The same glass etch was used (10:1:1 H₂O:HF:HNO₃) for 25 minutes in an ultrasonic bath. These die were then packaged and delivered.

4.0 Lessons learned

1. Better oversight at each step needed to ensure proper processing occurs
2. Polish before bond is critical for uniform plating across the wafer
3. Multiple operators who specialize in the processing phase should be employed rather than one operator for all steps. The lapping, plating, and bonding should be handled by experts.
4. Wetting must be confirmed before time is spent plating *vias*. Triton-X or a similar commercial product should be used
5. Because plating proved difficult, a group that specializes in plating (the LIGA group in 1725) should be consulted early in the process to ensure that the *vias* can be plated. As a parallel path, doing a liquid metal matrix fill and sintering for *via* fill should be considered.

5.0 *p*-Cresol – a uremic toxin and our target analyte:

Phenols are toxic, allergenic, carcinogenic and mutagenic compounds that are used in the manufacture of plastics, dyes, drugs, explosives, textiles, and pesticides [2, 3]. Cresols are substituted methylphenols (phenyl alcohols) and may be a model for monolignols (such as sinapyl, coniferyl or coumaryl aromatic alcohols) that are important in the biofuels arena [4]. Among the phenols, *p*-cresol (4-methyl phenol) has been studied extensively due to its role in uremic toxicity [5]. In addition to external sources of phenols, *p*-cresol also arises through tyrosine metabolism during protein breakdown by the gastrointestinal bacteria as well as from microbial actions on toluene or lignins [3]. We chose *p*-Cresol due to its role as a uremic toxin.

6.0 Electrochemical Detection of *p*-Cresol by two Investigators:

We next utilized the devices fabricated (*vide supra*) to detect our target analyte, *p*-Cresol. The reasons for involving two investigators for detecting *p*-cresol using electrochemical measurements were to demonstrate assay robustness, reliability and reproducibility.

6.1 Investigator # 1:

Twelve amine-coated gold micro-electrodes were obtained for *p*-cresol concentration curve measurements. Cyclic voltammetry was used to scan from -400mV to 900mV using a 100 mV/sec scan rate. The measurements were performed in a cell using 10 mL of 50mM Sodium Phosphate buffer (NaPB), pH 7.4; an Ag/AgCl reference electrode; and a platinum wire auxiliary electrode. Because of the radical formation created on the working electrode surface during *p*-cresol detection, each micro-electrode was used for only one measurement. Initial measurements

we taken for 50 mM NaPB (Sodium Phosphate buffer, no *p*-cresol), 1 nM *p*-cresol, 1 μ M *p*-cresol, 100 μ M *p*-cresol, 500 μ M *p*-cresol, and 1 mM *p*-cresol. The results are shown below:

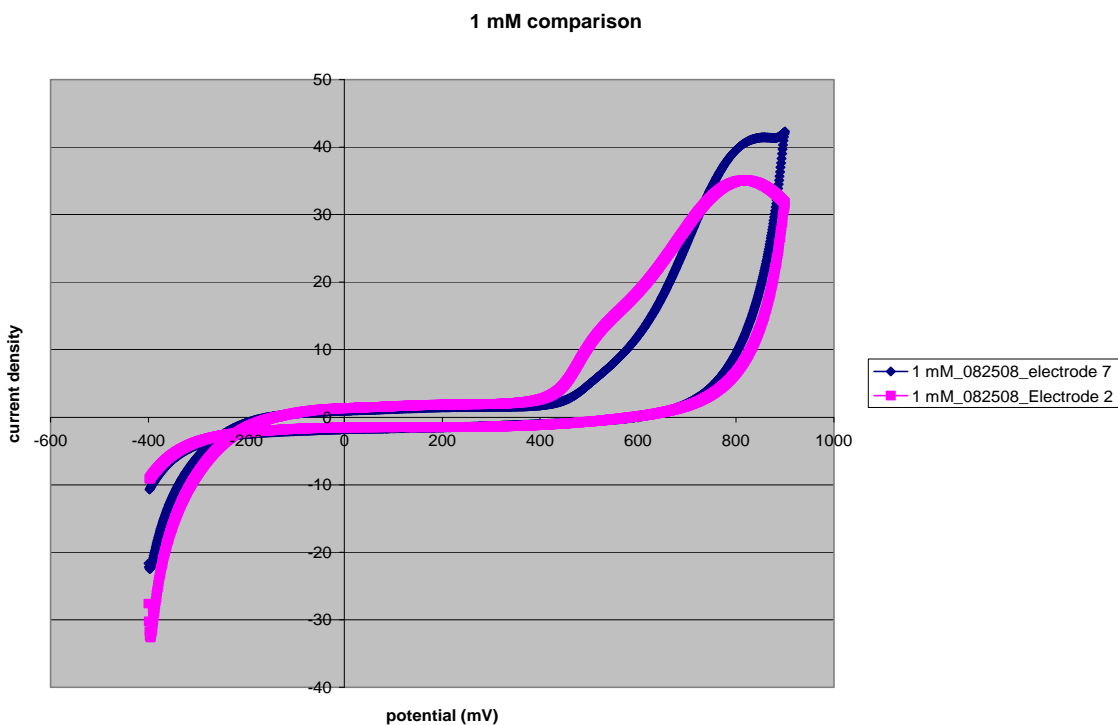


Figure 4A: 1mM *p*-Cresol electrochemical assay

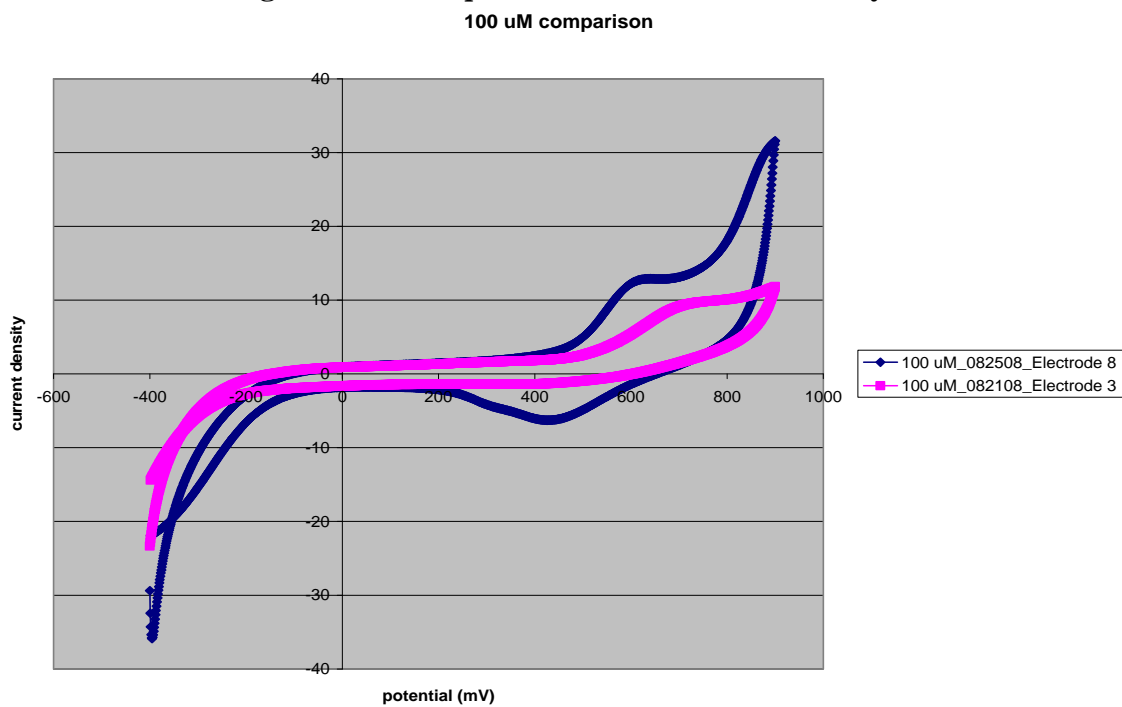


Figure 4B: 100 μ M *p*-Cresol electrochemical assay

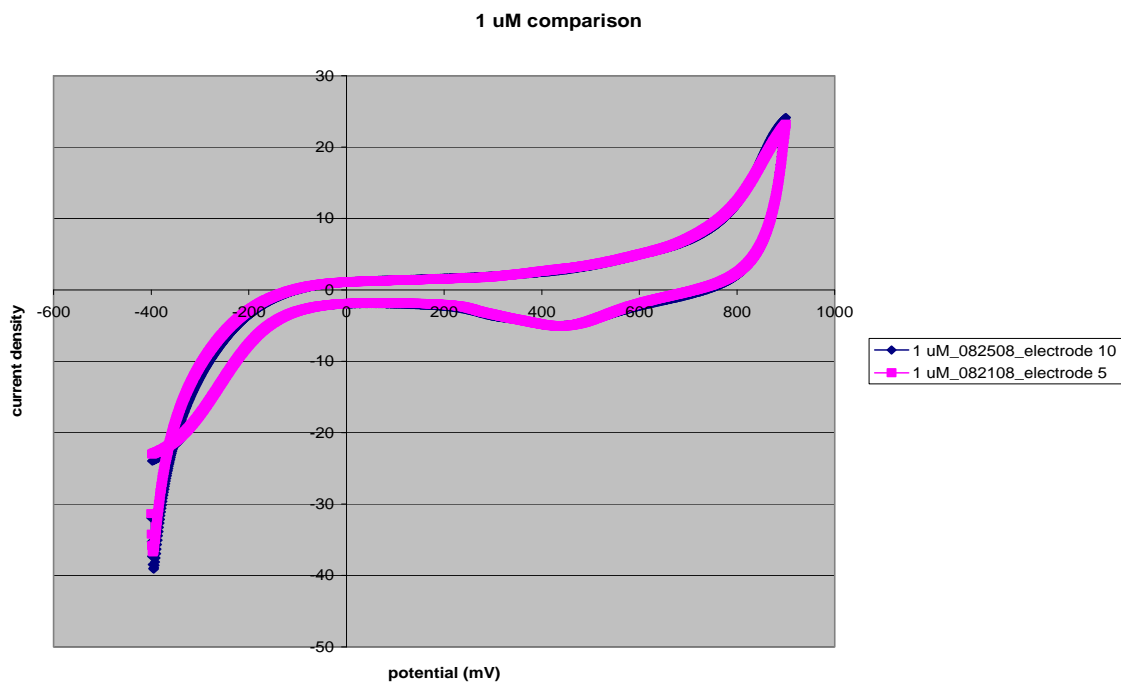


Figure 4C: 1 μM *p*-Cresol electrochemical assay

In efforts to better define a lower limit of detection a second concentration curve was obtained for 50 mM NaPB (no *p*-cresol), 1 nM *p*-cresol, 1 μM *p*-cresol, and 100 μM *p*-cresol. These results are shown below:

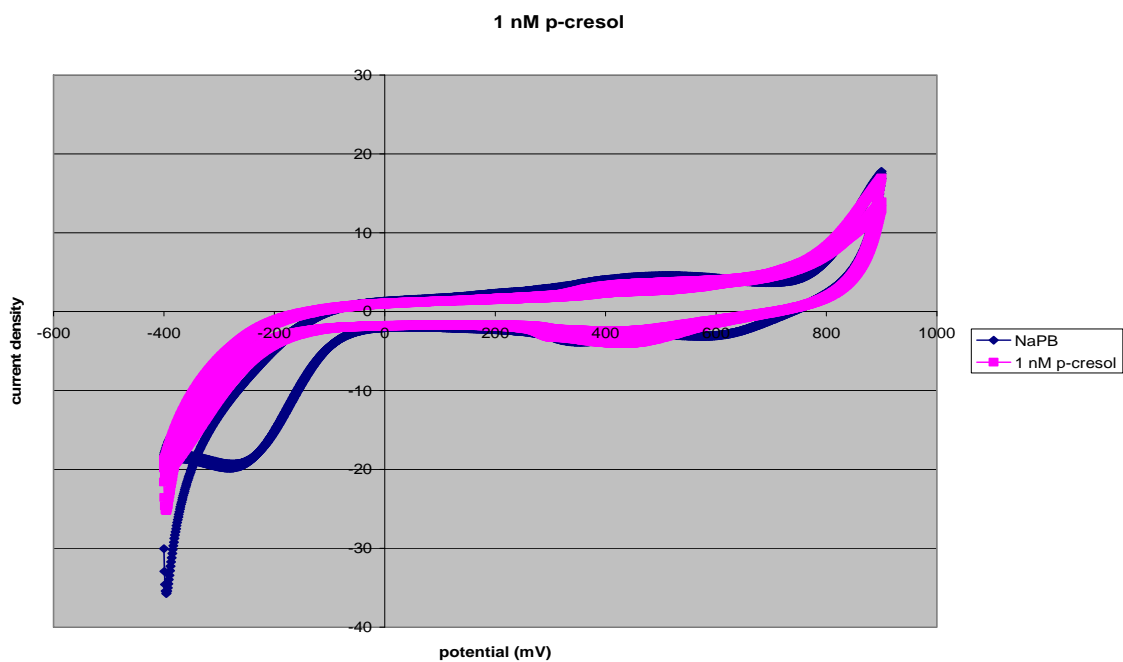


Figure 5A: 1 nM *p*-Cresol electrochemical measurements

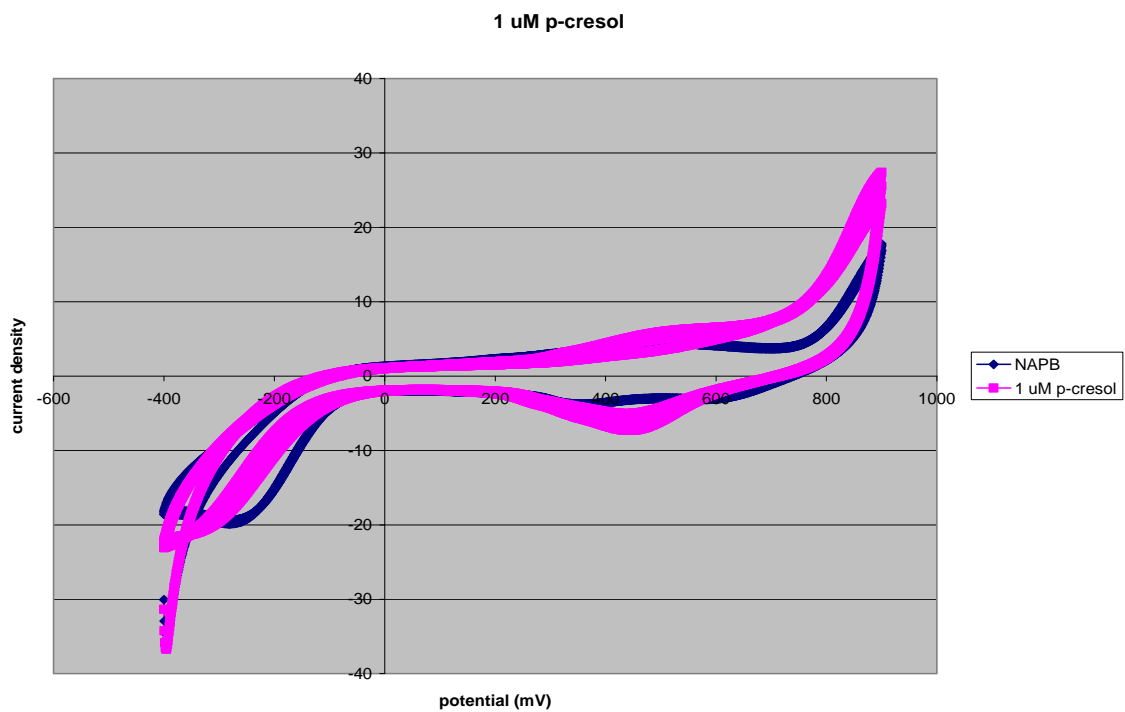


Figure 5B: 1 μM *p*-Cresol electrochemical measurements

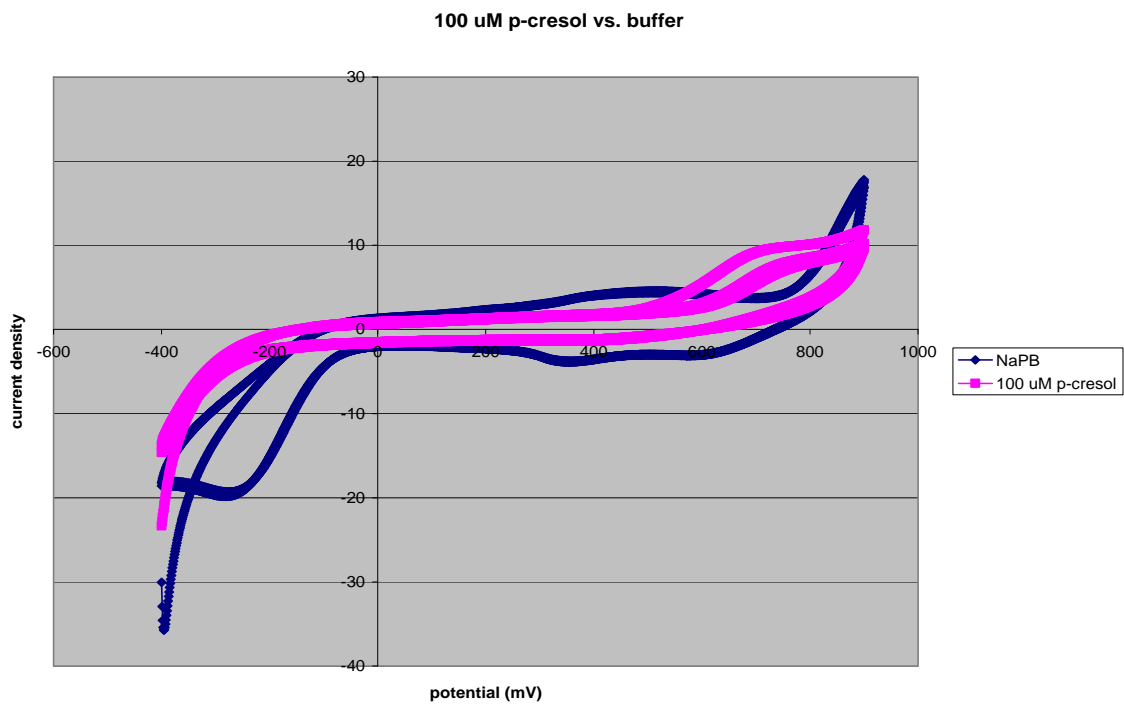


Figure 5C: 100 μM *p*-Cresol electrochemical measurements

Conclusions: These experiments demonstrated that *p*-Cresol could be detected using an electrochemical assay at a minimum threshold of 100 μ M.

6.2 Investigator # 2:

We next repeated *p*-Cresol electrochemical detection by a second investigator working separately in a different laboratory housed in a building about one-half mile away from the laboratory of Investigator # 1. These efforts were undertaken in order to demonstrate the robustness and reproducibility of our *p*-cresol assay using electrochemical measurements. The experimental details employed by the second investigator and the results are shown below:

Materials:

All aqueous solutions were prepared with 18 M Ω water using a Barnstead Nanopure water purifier (Boston, MA). Sodium phosphate monobasic, sodium phosphate dibasic, acetonitrile (ACN), *p*-cresol, and nitrobenzene diazonium were purchased from Sigma (St. Louis, MO). Tetrabutylammonium tetrafluoroborate (Bu₄NBF₄) was obtained from Aldrich. Sulfuric acid, ethyl alcohol (95% denatured), 30% hydrogen peroxide, and potassium chloride were purchased from Fischer Scientific (Pittsburgh, PA). Carboxylphenyl diazonium was synthesized according to known methods [6].

Electrochemical Instrumentation:

All electrochemical measurements were performed on a PGZ100 Voltalab potentiostat (Radiometer Analytical, Lyon, France) and were measured versus an Ag/AgCl reference (3M NaCl, aqueous solutions) or a Ag/AgNO₃ reference (10 mM, non-aqueous solutions, -102 mV vs. ferrocene couple) and a Pt counter electrode from Bioanalytical Systems (West Lafayette, IN). 5 mm diameter gold disk electrodes were prepared *via* thermal evaporation of a 200 \AA Ti adhesion layer followed by 2000 \AA of Au onto a Pyrex wafer. Au electrodes were cleaned immediately before use with freshly prepared piranha (5:3 conc. sulfuric acid: 30% H₂O₂) for 10 min, washed with nanopure water, and dried under a stream of nitrogen.

Electrode Functionalization:

Phenyl thin films were assembled onto clean gold electrodes *via* 2 cyclic voltammetry scans from 0 to -1 V in a solution of 1 mM nitrophenyl or carboxylphenyl diazonium salt and 0.1 M Bu₄NBF₄ in ACN. After electrodeposition, the electrodes were briefly rinsed with ACN, followed by a rinse with ethanol and a 15 second sonication in ethanol to remove any adsorbed phenyl diazonium. After sonication the electrodes were again rinsed in ethanol and dried under a stream of nitrogen. Aminophenyl films were obtained *via* the 6 electron electrochemical reduction of nitrophenyl groups to aminophenyl groups by cyclic voltammetry from -300 to -1300 mV in deoxygenated (argon sparge) ethanol:water (1:9) solution with 0.1 M KCl as supporting electrolyte.

Results and Discussion

p-Cresol can be oxidized at potentials between +500 to +800 mV vs. Ag/AgCl allowing for potentiometric electrochemical detection. The product of *p*-cresol oxidation is a highly reactive phenoxy radical species which polymerizes in solution near the electrode surface [7, 8]. This forms a passivating layer on the electrode within seconds, preventing reuse of the electrode. Many published reports of electrochemical detection of *p*-cresol utilize enzymes to metabolize *p*-cresol into a more electrochemically reversible analyte allowing reuse of the detector [9]. However, functionalization of Au electroneedles with enzymes was not pursued in this work as maintaining activity of the immobilized enzymes over several months would add significant complexity to the sensor design.

Effective electrochemical detection of *p*-cresol on carbon nanotube (CNT) modified glassy carbon electrodes (GCE) that resist passivation has been reported [10]. We therefore investigated methods for obtaining robust conducting thin films on Au surfaces with properties similar to those of carbon nanotubes. Phenyl films with various functional groups covalently linked to the Au surface *via* electroreduction of diazonium salts were selected for this study as the resulting phenyl surface may be similar to the phenyl surface of carbon nanotubes. In this approach the electrochemical reduction of a diazonium salt creates an aryl radical after the spontaneous elimination of dinitrogen, as shown in Figure 5. The resulting aryl radical can then form a covalent bond with conducting and semiconducting surfaces. This film is highly stable in terms of withstanding several minutes of ultrasonication and its long term storage in air, and remains conductive allowing for subsequent electrochemistry.

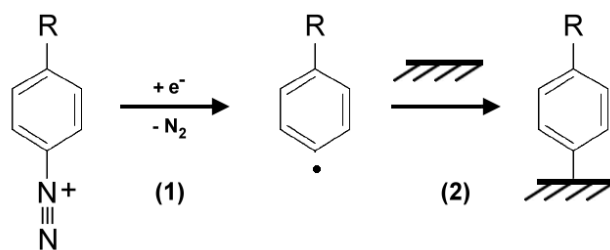


Figure 6. Mechanism of diazonium assembly onto electrode surfaces: 1) Electroreduction of the diazonium yielding a phenyl centered radical followed by 2) covalent grafting of the phenyl radical to the conducting or semiconducting substrate.

Electrochemical detection of *p*-cresol was initially performed on disposable 5 mm diameter Au disk electrodes. Phenyl films on Au with three differing functional groups, nitro, carboxyl, and amino were compared to the response obtained on a bare Au surface. Cyclic voltammograms of *p*-cresol in physiologically buffered sodium phosphate solution are shown in Figure 6. The bare gold surface (black) showed two oxidative waves near +500 and +735 mV vs. Ag/AgCl, similar to results published for electrochemical detection of *p*-cresol [10]. Oxidation of *p*-cresol on the nitrophenyl Au surface (red) showed a slightly reduced and positively shifted initial peak at +530 mV followed by an enhanced and negatively shifted peak

at +710 mV. The carboxylphenyl Au surface showed *p*-cresol oxidation currents at +510 and +660 mV with currents higher than both the bare and nitrophenyl Au surfaces. *p*-Cresol electrochemistry on the aminophenyl Au surface (blue) resulted in an initial oxidative peak nearly identical to that obtained from the nitrophenyl Au surface. However, the second oxidative wave at +770 mV showed significantly enhanced currents, more than twice the signal obtained from the other surfaces. The differences in acid-base pairing between the varying phenyl surfaces and the *p*-cresol may result in varying complementary π -donor-acceptor interactions leading to the observed differences in peak potentials and currents.

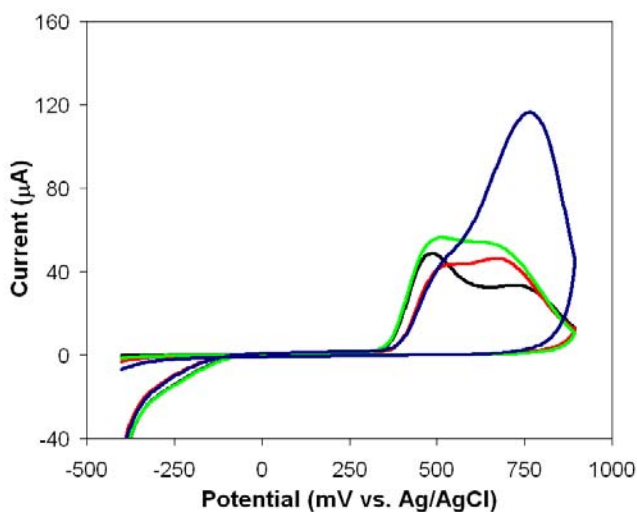


Figure 7. Cyclic voltammograms showing *p*-cresol oxidation at differing Au electrode surfaces: Black) unmodified Au; Red) nitrophenyl thin film Au; Green) carboxylphenyl thin film Au; Blue) aminophenyl thin film Au. 5 mM *p*-cresol in 50 mM sodium phosphate buffer, pH 7.4, scan rate = 100 mV/s.

Whether the phenyl modified Au surfaces could resist passivation was determined by performing 5 sequential CV scans in *p*-cresol solution. All surfaces were subject to passivation as highly diminished currents without any observable oxidative waves were obtained for scans 2-5. A typical result is shown in Figure 7 where following the first scan on an aminophenyl surface currents decreased from 116 μ A to 4 μ A and did not recover following washing and rinsing, or exposure to a fresh *p*-cresol solution. Although the mechanism for the resistance of the CNT modified GCE surface to passivation is not well understood, it is clear that a simple phenyl thin film does not adequately simulate the passivation resistive properties of a CNT-GCE surface. However, as point-of-care medical diagnostic measurements are the intended application of the electroneedle platform, re-use of the array may not be required. In this case, a single-use disposable array may be more desirable.

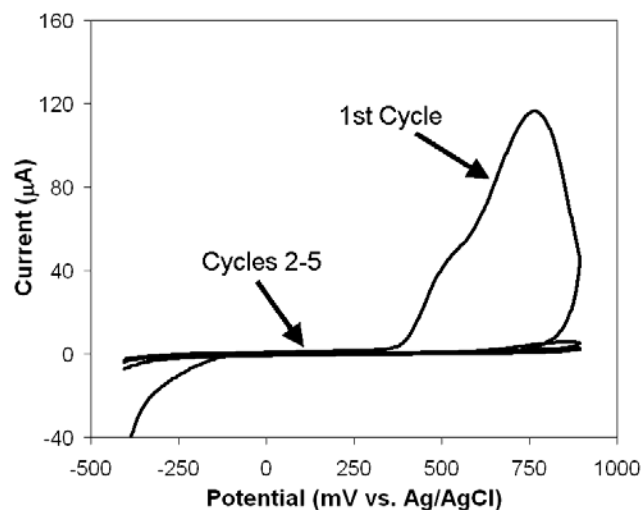


Figure 8. Sequential cyclic voltammograms scans of an aminophenyl thin film modified Au electrode. 5 mM *p*-cresol in 50 mM sodium phosphate buffer, pH 7.4, scan rate = 100 mV/s.

Electrochemical detection of *p*-cresol levels in physiologically buffered sodium phosphate solution were measured at aminophenyl Au surfaces as this thin film modification resulted in the highest current signal. The current response obtained at +770 mV over concentrations of 1 mM to 100 nM is shown in Figure 8. These data show that the electrochemical assay is quantitative and has a detection limit in the very low μM regime.

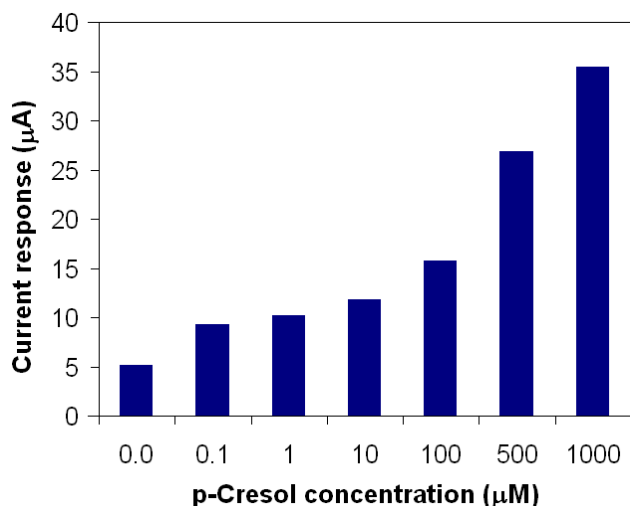


Figure 9. Oxidative *p*-cresol detection at an aminophenyl thin film modified Au electrode. Reported currents were obtained at +770 mV vs. Ag/AgCl from cyclic voltammetry in a 50 mM sodium phosphate buffer solution, pH 7.4, scan rate = 100 mV/s.

7.0 *p*-Cresol Detection Using Enzyme Catalysis:

We next attempted an orthogonal fluorescence assay for *p*-Cresol in order to validate the electrochemical measurements. Laccases (benzenediol:oxygen oxidoreductase, E.C. 1.10.3.2) catalyze the oxidation of phenols, substituted phenols as well as non-phenolic substrates, while reducing atmospheric molecular oxygen to water [11-13]. During oxidation, the corresponding four phenoxy radicals that are produced undergo non-enzymatic reactions including radical coupling and polymerization [14-16] resulting in 2, 2'-dihydroxy-5,5'-dimethylbiphenyl and 4 α -9 β -dihydro-8,9- β -dimethyl-3(4H)-dibenzofuranone (Pummerer's ketone) [17, 18]. We therefore developed a new spectroscopic analysis of *p*-Cresol that was oxidized by a fungal (*Trametes versicolor*) laccase. The assay is flexible since the same reaction can be interrogated using absorption and fluorescence under acidic or basic pH reaction conditions in real time (kinetic) or endpoint modes. Our assay may be useful in the triage of dialysis patients.

8.0 Fluorescent Properties of Oxidized *p*-Cresol:

We first investigated the excitation and emission profiles of the oxidation products of laccase-catalyzed oxidation of *p*-Cresol. The results are shown below.

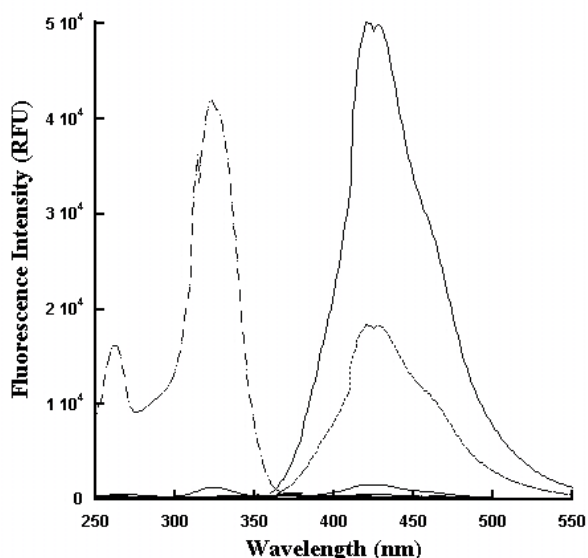


Figure 10. Excitation and emission profiles of the laccase-catalyzed oxidation products of *p*-cresol. Reaction samples mixed with 50mM NaOH were subjected to fluorescence spectroscopy. The dashed tracing showing the double peaks (left) is the excitation profile with emission fixed at 425nm. The solid large peak (right) represents the emission profile with excitation fixed at 322nm. The smaller dotted peak (right) represents the emission profile with excitation fixed at 262nm. The various “control” tracings of buffer only, laccase only and *p*-cresol only are shown hugging the abscissa. Two very small intrinsic fluorescence peaks from *p*-cresol alone (i.e., without laccase) were noted at λ_{max} of 322nm and 425nm, respectively.

We next used the laccase-oxidation of *p*-cresol to determine assay sensitivity. In this experiment, increasing concentrations of *p*-cresol was reacted with laccase and the fluorescence of the oxidation products was measured. The results are shown in Figure 10.

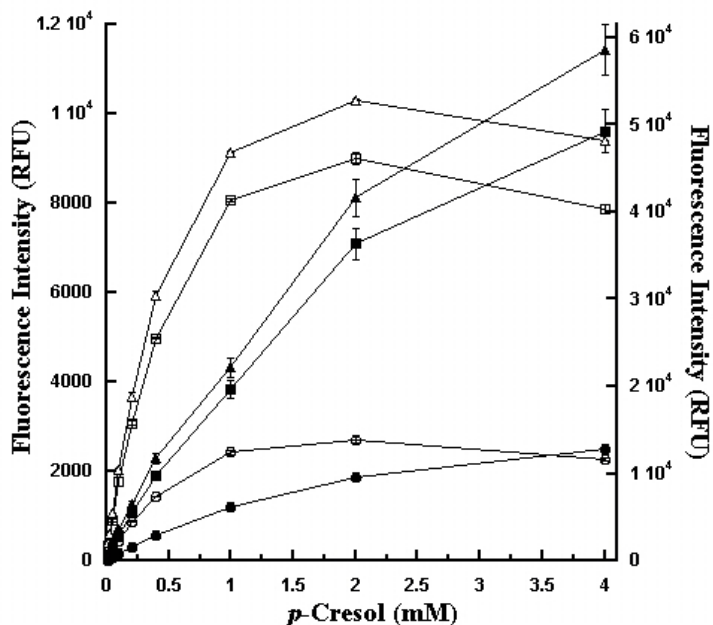


Figure 11. *p*-Cresol affinity for laccase. Increasing and indicated concentrations of *p*-cresol were reacted with 100pg/ μ L laccase (open and closed circles), 500pg/ μ L laccase (open and closed squares) and 1000pg/ μ L laccase (open and closed triangles). After 30 minutes at 37°C, the reactions were terminated by the addition of 50mM NaOH (final) and the fluorescence emission was monitored by λ_{ex} , 262nm / λ_{em} , 425nm (open symbols; left-Y axis) or λ_{ex} , 322nm / λ_{em} , 425nm (closed symbols; right-Y axis).

9. Concluding Remarks

This LDRD project made significant progress and reached important milestones. These were as follows: 1) A concentration of 10 μ M *p*-cresol was detected by laccase catalysis. 2) Detection was accomplished rapidly, within two minutes (Figure 10). 3) 1 to 10 μ M *p*-cresol was detected by electrochemical measurements. 4) The sensitivity of *p*-cresol detection by our methods was thus 1ppm (50ng; 1080 μ g/L). 5) We demonstrated orthogonal detection using electrochemical and fluorescence measurements. 6) Depending upon the amount of laccase and reaction time, concentrations of *p*-cresol lower than 10 μ M were potentially detectable. Our data are in agreement with *p*-cresol detection limits of 15ng [19], 21-24ppm [20], and 1.0–5.3 μ M [21] reported previously. Our values for *p*-cresol detection are also within an order of magnitude sensitivity reported earlier based upon the direct fluorescence emission from *p*-cresol [22-24].

We thus demonstrated two orthogonal assays for *p*-Cresol, a uremic toxin, using a Medically Relevant ElectroNeedles technology and a High-Throughput Screening (HTS) technology. Valuable lessons were learned during fabrication of these devices. Orthogonal assays improve the sensitivity and specificity of *p*-cresol detection especially during medically relevant/urgent situations. Our assays may be valuable for the triage of dialysis patients.

10.0 REFERENCES

1. U. Kreibig, *Applied Physics*, **1976**, 10, 255.
2. Veeresh, G. S.; Kumar, P.; Mehrotra, I. *Water Res.*, **2005**, 39, 154.
3. Peters, F.; Heintz, D.; Johannes, J.; van Dorsselaer, A.; Boll, M. *J. Bacteriol.*, **2007**, 189, 4729.
4. Han, K-H.; Ko, J-H.; Yang, S. H. *Biofuels, Bioprod. Bioref.*, **2007**, 1, 135.
5. Vanholder, R.; De Smet, R.; Lesaffer, G. *Nephrol. Dial. Transplant.*, **1999**, 14, 2813.
6. McNab, H., Monohan, L. C. *J. Chem. Soc. Perkin. Trans.: Org. Bio-Org. Chem.*, **1989**, 1, 419.
7. Wang, J., Jiang, M., Lu, F. *J. Electroanal. Chem.*, **1998**, 444, 127.
8. Wang, J., Martinez, T. *J. Electroanal. Chem.*, **1991**, 313, 129.
9. Rogers, K. R., Becker, J. Y., Cembrano, J. *Electrochim. Acta*, **2000**, 45, 4373.
10. Wang, J., Deo, R. P., Musameh, M. *Electroanalysis*, **2003**, 15, 1830.
11. Johannes, T. W.; Woodyer, R. D.; Zhao, H. In *Enzyme Assays: High-Throughput Screening, Genetic Selection and Fingerprinting*; Raymond, J-L. Ed.; Wiley-VCH, Verlag GmbH & Co., Weinheim, **2006**; pp. 77-93.
12. Baldrian, P. *FEMS Microbiol. Rev.*, **2006**, 30, 215.
13. Kunamneni, A.; Ballesteros, A.; Plou, F. J.; Alcalde, M. In *Communicating Current Research and Educational Topics and Trends in Applied Microbiology*; Mendez-Vilas, A. Ed.; Formatex, Badajoz, Spain, **2007**; Volume I, pp. 233-245.
14. Hewson, W. D.; Dunford, H. B. *J. Biol. Chem.*, **1976**, 251, 6043.
15. Raven, E. L.; Celik, A.; Cullis, P. M.; Sangar, R.; Sutcliffe, M. *J. Biochem. Soc. Trans.*, **2001**, 29, 105.
16. Kobayashi, S.; Higashimura, H. *Prog. Polym. Sci.*, **2003**, 28, 1015.
17. Liu, Z.; Cai, R.; Mao, L.; Huang, H.; Ma, W. *Analyst*, **1999**, 124, 173.
18. Celik, A.; Cullis, P. M.; Lloyd, E. R. *Arch. Biochem. Biophys.*, **2000**, 373, 175.
19. Yoshikawa, M.; Taguchi, Y.; Arashidani, K. *J. Chromatogr.*, **1986**, 362, 425.
20. Rogers, K. R.; Becker, J. Y.; Wang, J.; Lu, F. *Field Anal. Chem. & Technol.*, **1999**, 3, 161.
21. Solna, R.; Sapelnikova, S.; Skladal, P.; Winther-Nielsen, M.; Carlsson, C.; Emneus, J.; Ruzgas, T. *Talanta*, **2005**, 65, 349.
22. Niwa, T. *Clin. Chem.*, **1993**, 39, 108.
23. Smet, R. D.; David, F.; Sandra, P.; Kaer, J. V.; Lesaffer, G.; Dhondi, A.; Lameire, N.; Vanholder, R. *Clin. Chim. Acta*, **1998**, 278, 1.
24. Martinez, A. W.; Recht, N. S.; Hostetter, T. H.; Meyer, T. W. *Am. Soc. Nephrol.*, **2005**, 16, 3430.

11. Distribution

#	Mail Stop	Name	Org #
1	MS-0899	Technical Library	9536 (electronic copy)
1	MS-0123	Donna Chavez, LDRD Office	1011 (electronic copy)
1	MS-1425	Komandoor Achyuthan	1714 (electronic copy)

